8th European Workshop On Structural Health Monitoring (EWSHM 2016), 5-8 July 2016, Spain, Bilbao
www.ndt.net/app.EWSHM2016

Application of Biaxial FBG Sensors to Monitor Poisson's Ratio of Composites as Damage Index

Cagatay Yilmaz[1], Cagdas Akalin[1], Esat Selim Kocaman[1], Afzal Suleman[2], MehmetYildiz[1*]

[1]Faculty of Engineering and Natural Sciences, Integrated Manufacturing Technologies Research and Application Center, Sabanci University, 34956, Istanbul, Turkey
* meyildiz@sabanciuniv.edu

[2]Department of Mechanical Engineering, Center for Aerospace Research
University of Victoria, Victoria, BC, V8W 3P6 CANADA

Abstract

Damage accumulation in Glass Fiber Reinforced Polymer (GFRP) composites is monitored based on Poisson's ratio measurements for three different fiber stacking sequences subjected to both quasi-static and quasi-static cyclic tensile loadings. The sensor systems utilized include a dual-extensometer, a biaxial strain gage and a novel embedded-biaxial Fiber Bragg Grating (FBG) sensor. These sensors are used concurrently to the measure biaxial strain whereby the evolution of Poisson's ratio as a function of the applied axial strain is evaluated. It is observed that each sensor system indicates a non-constant Poisson's ratio, which is a sign of damage accumulation under the applied tensile loading. As the number of off-axis plies increases, transverse strain indicates a notable deviation from linearity due to the formation of transverse cracking, thereby leading to a larger reduction in Poisson's ratio as a function of applied axial strain. Here, it is demonstrated that biaxially embedded FBG sensors are reliable to monitor the evolution of Poisson's ratio, unlike biaxial strain gages which record strain values that can be significantly influenced by the cracks formed on the surface of the specimen.

Keywords: Poisson's ratio; Transverse cracking; Stress transfer; Glass fibers; Fiber Bragg Grating

1. Introduction

Glass or carbon fiber reinforced polymeric composites have received a great deal of attention due to their high specific strength and stiffness for structural applications. The relatively high specific strength of composite materials makes them suitable for applications where the weight and operating costs are intimately coupled. In comparison to metallic materials, where the failure is usually triggered by a single crack during their service life, composite materials exhibit poorly characterized damage mechanisms due to the existence of multiple cracks, which makes the prediction of service life rather complex and difficult. Therefore, in literature, there are several approaches developed and investigated to understand the accumulation of damage and damage state of composite structures under static and dynamic loading conditions. For example, Highsmith and Reifsnider studied stiffness reduction as a damage indicator in composite materials [1]. Several researchers examined the reduction of Poisson's ratio as a damage indicator [2-5] since Poisson's ratio ($\nu_{xy}=-\varepsilon_y/\varepsilon_x$) embodies both axial and transversal strain (ε_x and ε_y, respectively) information and is affected by the transverse cracks formed as a result of applied longitudinal strain [6-8]. Paepegem et al. [6] investigated the evolution of Poisson's ratio of composite materials as a function of applied longitudinal strain, and showed that Poisson's ratio decreases by the applied strain. Smith et al.[8] modelled the evolution of Poisson's ratio using a shear-lag theory under static loading conditions, correlated their analytic model with experimental results, and indicated that Poisson's ratio decreases as the transverse crack density increases.

The measurement of Poisson's ratio of composites subjected to dynamic and static loading has mainly been performed using strain gages and extensometers. Due to their size, these sensors cannot be embedded in composite structures, and thus measure the strain from the surface. Additionally, surface mounted strain gages detach easily under cyclic loading, even at relatively few cycles. Moreover, strain gage and extensometer are sensitive to electromagnetic interference, and hence cannot be used in environments with high electromagnetic interference. To circumvent the drawbacks of strain measurements with surface mounted electrical strain sensor systems, one promising approach is the utilization of embedded Fiber Bragg Grating (FBG) based sensor systems [9]. FBG is a section of a single mode optical fiber which contains a periodic variation of refractive index formed holographically on the core of the optical fiber along the fiber direction, and acts like a stop-band filter [10, 11]. An FBG sensor reflects a small portion of the incoming electromagnetic spectrum while enabling the passage of the others. The center wavelength of the reflected portion of the incident electromagnetic spectrum is referred to as the Bragg wavelength, $\lambda_B = 2n_{eff}\Lambda$ where Λ is grating period and n_{eff} is the effective refractive index of the FBG sensor. When subjected to strain or temperature variations, the grating period and the effective refractive index of the FBG sensor change, thereby causing a shift in the Bragg wavelength λ_B. The change in the Bragg wavelength can be coupled to external effects, namely, temperature and strain through the following equation $\Delta\lambda_B / \lambda_B = (\alpha + \xi)\Delta T + (1-\rho_e)\varepsilon$ where α and ξ are the thermal expansion and thermo-optic coefficients of the fiber core, respectively. Here, $\Delta\lambda_B$ is the shift in the Bragg wavelength, ΔT is the change in the temperature of the grating region and ρ_e denotes effective photo-elastic constant of the fiber core, which is taken as 0.22 in this work, and ε is the axial strain of the grating region. For a constant temperature, one can write the previous relation as $\Delta\lambda_B / \lambda_B = (1-\rho_e)\varepsilon$.

In this study, we have investigated the effect of transverse cracking on the reduction of Poisson's ratio as a function of imposed axial strain. To this end, composite specimens with three different ply stacking sequences (i.e., uniaxial laminates, and laminates with two and four 90^o off-axis plies) are instrumented with a biaxial extensometer and strain gage and then subjected to a quasi-static loading, thereby shedding light on the intimate relation between the reduction in Poisson's ratio and the off-axis/transverse ply cracking. Given that, in angle ply composites, the deformation in the lateral direction is enhanced, which can easily obscure the effect of transverse cracks on the lateral deformation, we limit our study to laminates with 0^o and 90^o stacking orientations. A novel approach for embedding biaxial FBG sensor into a composite laminate is proposed and utilized for multi-axis strain acquisition as well as for structural health monitoring of composites through referring to the reduction in Poisson's ratio. Specimens with extensometer, strain gage and embedded biaxial FBG sensor are subjected to quasi-static cyclic loading to study the reduction in Poisson's ratio under cyclic loading. It is shown that there can be notable variation in the values of lateral strain recorded by extensometer, strain gage and FBG sensor due to the difference in the gage length of these strain sensors. Referring to the reduction in Poisson's ratio, it is shown that composite specimens with a higher number of off-axis plies are more prone to the formation of transverse cracks. This study contributes to the state of the art in the field of composites materials testing and it is the first reported study on the measurement of decline in Poisson's ratio for composites with different fiber stacking sequences using embedded biaxial FBG sensors.

2. Methodology

The fiber reinforcement consists of 330gsm uni-directional (0^o) E-glass stitched fabric (Metyx, Turkey) with the trade code of L300 E10B-0. The matrix material is Araldite LY 564 epoxy and XB3403 hardener system purchased from Huntsman. Glass fibers were impregnated with resin by using vacuum infusion and then cured at 75 ^{o}C for 15 hours. In this study, three composites laminates with the fiber stacking configurations of [90/90/0]s, [90/0/0]s, [0]6 were manufactured, which are respectively denoted by G6B1, G6B2, and G6U1 for convenience. In this study, we have used dual FBG sensors (purchased from Technesa with λ_B=1540 nm (transversal) and λ_B=1550 nm (axial) and a gage length of 1 mm written holographically within the core of a polyimide coated single mode fiber such that the distance between both FBG sensors is nearly 21 cm. The optical cable with dual FBG sensors is fixed to the dry ply before composite manufacturing by interlacing it through stitching fibers of the ply in a configuration. The ply with FBG sensors is stacked such that FBG sensors are embedded into the symmetry axis of laminates during the manufacturing stage. The panel including the FBG sensor is cut into a L-shape so that the specimen can be clamped by the wedge grips of the universal machine without damaging the egress region of the FBG sensor. The egress/ingress of the optical cable into the composite was described in our previous study [12].

All static tensile tests were performed using a Zwick Z100 universal testing machine with a ± 100 kN load cell . Static tensile tests on composite specimens with or without embedded biaxial FBG sensors were conducted under the displacement control of 2 mm/min according to ISO 527 standard. A Micron Optics SM230 model interrogator was used to acquire the FBG signals with a sampling frequency of 1000 Hz during the experiments with Micron Optics Enlight Software. General purpose biaxial strain gages purchased from Micro-Measurements are used as axial and biaxial sensors with the code of C2A-06-062LW-350 and C2A-06-062LT-350, respectively. All the strain gages have a gage length of ~1.57 mm (0.062 inche) and a resistivity of 350 ohms. An Epsilon 3542 axial extensometer with a fixed gage length of 25 mm and an Epsilon 3575 transverse extensometer with a controllable gage length were utilized during tensile tests. Extensometer and strain gage data were collected concurrently by a National Instruments NI SCXI-1000 main chassis with a NI SCXI-1520 card at a sampling frequency of 1000 Hz.

3. Results and Discussion

3.1. Quasi-Static Tensile Tests

3.1.1 The Effect of Stacking Sequence on the Evolution of Poisson's Ratio

In order to assess the evolution of Poisson's ratio of composite plates with different stacking sequences, test specimens were subjected to quasi-static tensile loading until failure and all the data collected during the tests were processed and tabulated in Table 1 along with the fiber volume fractions. During the quasi-static tensile tests of all composite coupons, both axial and transversal strains were recorded by extensometers. Biaxial strain gages were attached only to a single coupon for each plate to investigate the effect of sensor type (i.e., gage length, measurement location) on the strain measurement. Figure 1(a) yields stress-strain curves for composite coupons having different stacking sequences. One can see from Table 1 that, as the number of 0^o layer increases, so do the strength and elastic modulus of composites, as expected. It is observed that the axial strain at failure does not differ significantly for composites with three different stacking sequences. Considering the iso-strain condition, strain of fibers, composite and matrix must be same at break, namely, $\varepsilon_c = \varepsilon_f = \varepsilon_m$. The fact that the failure of the composite takes place at the ultimate strain of the fibers parallel to the loading direction explains why composites with different stacking orientations have nearly the same axial strain. On the other hand, as seen in both Figure 1(b) and Table 1, on increasing the amount of 90^o fibers (perpendicular to loading), the ultimate transverse strain of the composite decreases due to the fact that 90^o fibers increase the elastic modulus of the composite in the transversal direction.

Table 1: Mechanical properties of composites with three different stacking configurations (strain measurements are based on extensometer).

	G6U1 $[0]_6$	G6B2 $[90/0/0]_s$	G6B1 $[90/90/0]_s$
Strength (σ_u) MPa	716	508	310
Elastic Modulus (GPa)	28	20	15
Axial Strain (ε_x) ($\mu\varepsilon$)	26175	26500	25739
Transverse Strain (ε_y) ($\mu\varepsilon$)	5363	2578	1334

Fiber Volume Fraction (v_f) (%)	41.3	38.1	42
Maximum Poisson's ratio	0.253	0.167	0.113
Minimum Poisson's ratio	0.203	0.095	0.051
Percent change (%) in Poisson's ratio	19	41	54.3

Poisson's ratios for three different stacking sequences are calculated using experimental data collected by dual extensometers during quasi-static tensile tests and are also given in Table 1. Figure 1(c)-(d) presents the variation of extensometer and strain gage based Poisson's ratio as a function of the axial strain for three different stacking configurations. Here, the plot for each stacking sequence is associated with the result of one of the five tests performed for a given stacking orientation. It is observed that the Poisson's ratio sharply increases with rise in the axial strain and reaches a maximum point, which will be hereafter referred to as the maximum Poisson's ratio. Thereafter, it decreases continuously until failure of the specimen. The Poisson's ratio at failure point is termed the minimum Poisson's ratio. The initial increase in the Poisson's ratio can be explained such that, at the early stages of the experiment, the transversal strain varies nonlinearly with respect to the axial strain, as can be seen in Figure 1(b). Hence, the increase in the axial strain as the test continues generates a larger increase in the lateral strain whereby the Poisson's ratio increases and reaches a maximum. Referring to Figure 1(c)-(d), one can immediately note that, as the number of 90^o plies increases, the composite specimen has smaller maximum and minimum Poisson's ratio, which is due to the higher elastic modules of off-axis plies than the matrix.

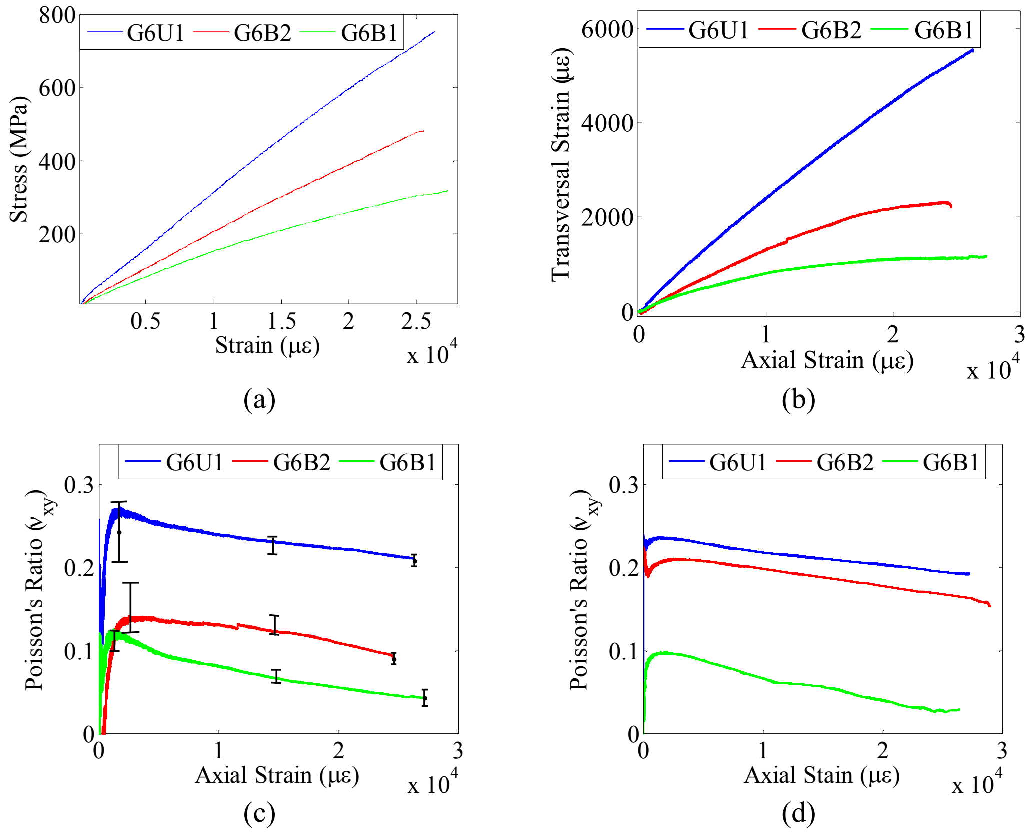

Figure 1: A representative stress-strain (extensometer) curve (a), the variation of extensometer based transverse strain as a function of axial strain for composite with three different stacking sequences (b), and the evolution of Poisson's ratios with respect to axial strain measured by extensometers and strain gages, respectively (c)-(d).

In reference [5], the decrease in the Poisson's ratio was associated with the enhancement of the elongation of the composite specimen due to the formation of transverse cracks under tensile loading, such that the specimen elongates further in the loading direction, hence causing a continuous decrease in the Poisson's ratio. If the axial elongation was notably influenced by the transverse crack density, one would expect higher elongation as the number of 90° plies increased given that, the higher the number of off-axis plies, the bigger the transverse crack density. However, as seen from Table 1, all three different stacking configurations have nearly the same axial strain at the failure. We suggest that the decreasing trend in Poisson's ratio is associated with the reduction in the rate of increase of the lateral strain due to transverse cracking. Knowing that transverse cracking will reduce the transfer of axial stress to the lateral direction, the specimen should experience a progressively smaller increase in the lateral strain with applied load as the test continues. It would be prudent to expect that, the larger the number of 90^{o} plies, the bigger would be the drop in the Poisson's ratio, as can be seen from Table 1. This bespeaks that the nearly linear decrease in the Poisson's ratio as a function of applied axial strain is directly controlled by the density of transverse cracking.

3.2 Quasi-Static Cyclic Loading

3.2.1 Damage Accumulation

Three composite laminates with three different stacking sequences (i.e., G6U1, G6B2, and G6B1) were manufactured with embedded biaxial FBG sensors and then cut into tensile specimens. These specimens were instrumented with a biaxial strain gage, biaxial FBG sensor, and axial and transversal-extensometer, and then subjected to quasi-static cyclic tensile testing with a load increment of 50 MPa after each complete cycle until failure. During the initial loading cycle, certain damage modes such as transverse cracking, delamination and splitting occur. In the subsequent loading cycles, the damage created in previous cycles accumulates. Therefore, the quasi-static cyclic test enabled us to examine the effect of axial strain level on the damage state and accumulation in composites, thereby revealing the efficacy of monitoring Poisson's ratio for following the damage state of composite materials. The loading history of a test specimen as a function of displacement and time is given in Figure 2(a)-(b), respectively, for G6B1.

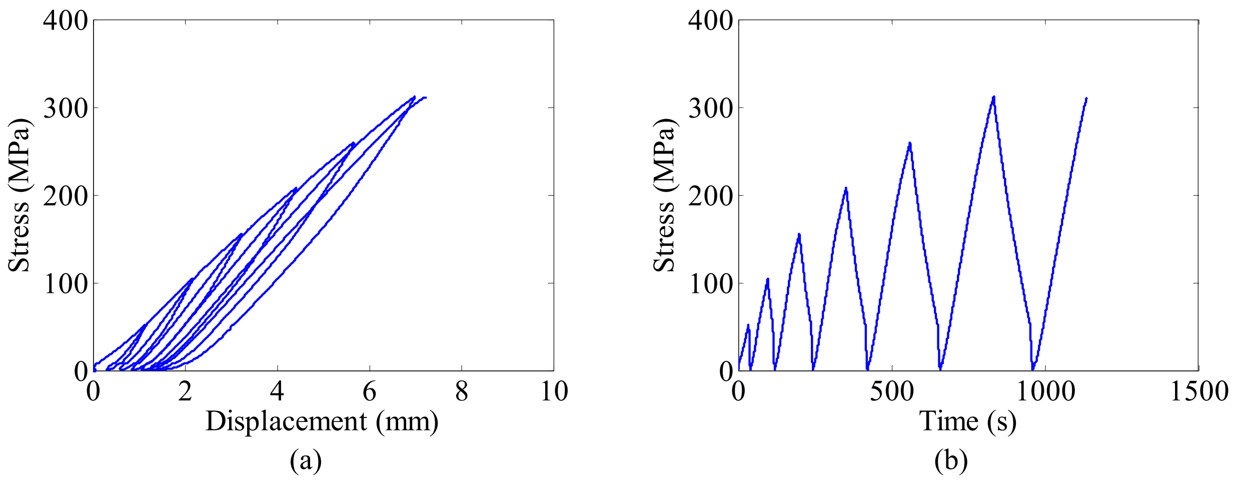

Figure 2: The loading history of a test specimen instrumented with surface mounted bi-axial strain gage, dual extensometer, and embedded bi-axial FBG sensor for G6B1.

To show the formation of transverse cracks during the quasi-static cyclic tension test, the tensile experiment on G6B1 specimen was recorded in a video using a Nikon D7100 camera with a macro lens while the specimen with a black background was subjected to a white light source. Figure 3 presents image frames extracted from the video for different stress levels. At lower stress levels up to 100 MPa, transverse cracks are not visible, but the color of the specimen changes gradually to blurry white since micron or submicron cracks alter the refractive index of the specimen. When the stress increases up to 150 MPa, cracks become visible and the color of the specimen completely turns to milky white since the rise in crack density scatters the light more thereby causing a color shift in the specimen. As the stress continues to increase further, transverse cracks become more visible, and the color of the specimen gets milkier due to scattering of light by small cracks. After the failure of the specimen, there is a noticeable reduction in the white contrast and visibility of the cracks with respect to the previous frame, which can be attributed to the removal of the load from the sample due to breaking, resulting in the closure of some open cracks.

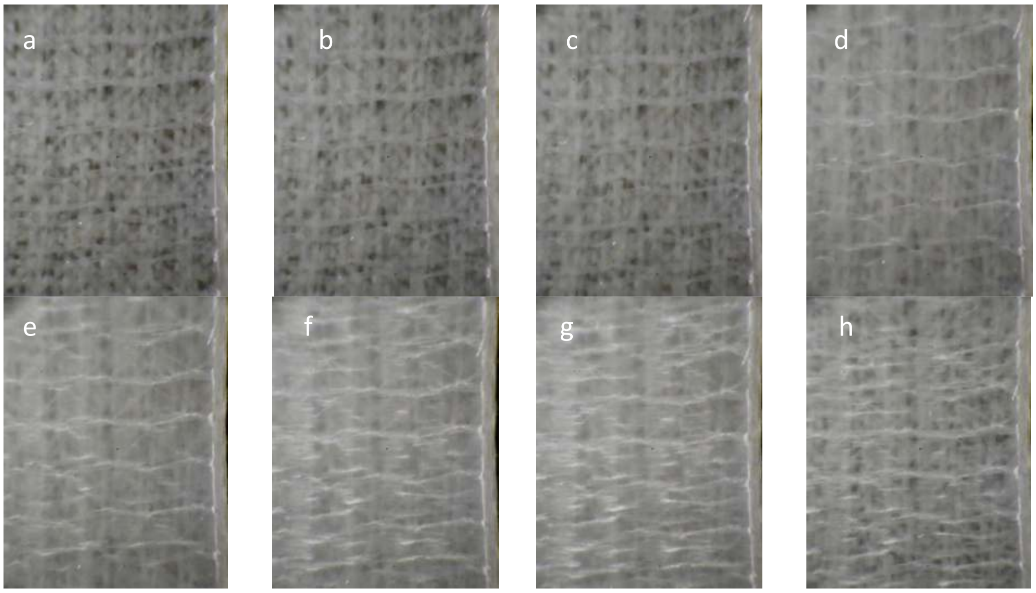

Figure 3: The deformation of a test specimen from the G6B1 laminate which was recorded by a macro lens attached to a camera; a) 0 MPa load, b) 50 MPa, c) 100 MPa, d) 150 MPa, e) 200 MPa, f) 250 MPa, g) 280 MPa (just before failure), and h) just after breakage.

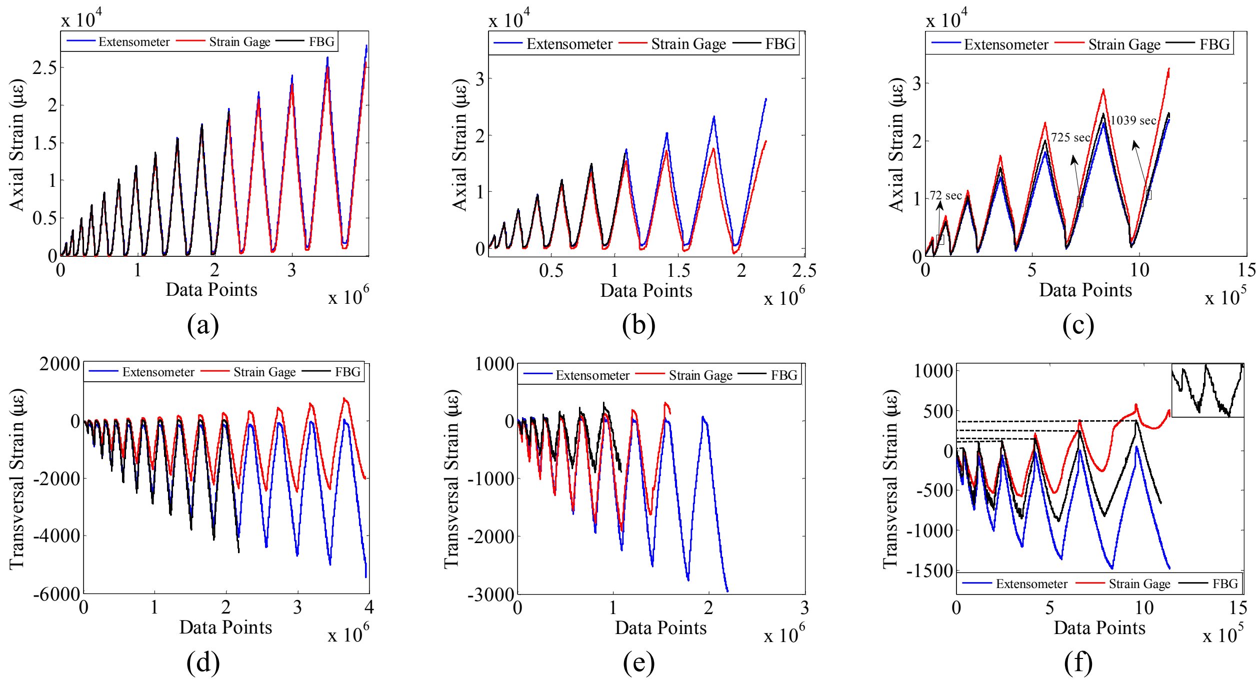

Figure 4: The variation of axial and transversal strains recorded by three different sensor systems for three dissimilar stacking sequences namely, G6U1, G6B2, and G6B1, given in column-wise ordering.

The variations of axial and transverse strains measured simultaneously by extensometer, strain gage and FBG sensor during the quasi-static cyclic tensile tests are provided in Figure 4. As one can note from Figure 4(a)-(c), in the first loading cycle, all three sensors measure nearly the same axial strain values for three stacking sequences, albeit with minor differences. It is interesting to note that the axial strain values recorded by three different sensor systems for specimens with off-axis plies start deviating from each other as the cycle number increases. These deviations start at earlier cycles for the specimen with four off-axis plies in comparison to that with two off-axis plies. As for the specimen without off-axis plies, all three sensors have a negligible difference in the acquired axial strains during the entire loading history. This indicates that composites with off-axis plies are quite prone to the formation of transverse cracks which are known to alter the strain state within specimens, whereby different sensors read slightly dissimilar values. In other words, locally and globally measured strains can differ from each other owing to the difference in the gage length of the sensors used and the crack density and the orientations in the proximity of these sensors. The upward shift in the trough of the axial strains of all sensors under zero loading in Figure 4(a)-(c) is due to the permanent damage in the composite specimen. Figures 4(d)-(f) show that three different sensors measure nearly the same maximum lateral strain for the very early cycles, even in the composites with different stacking sequences. On the formation of transverse cracks, the lateral strain state in the composite changes significantly. So far, it has been understood that the density of transverse cracks is larger in composites with 90^o plies than with 0^o plies, and thus the local permanent deformation due to the transverse cracking is expected to be smaller in G6U1. Hence, the local lateral strain measured by the FBG sensor is very much the same as that collected by surface mounted extensometer, as seen in Figure 4(d). One can see from Figure 4(e)-(f) that the strain readings of sensors with smaller gage length notably deviate from the extensometer in composites with off-axis plies. This is not due to the malfunctioning of any sensors; it is rather related to the damage state in the vicinity of the sensors and their gage length. Extensometers, due to their larger gage length, measure average strain in comparison to strain gage and FBG sensors and, therefore, in the structures prone to local damage formation, the readings of sensors with smaller gage length can be different, and also this difference is further enhanced depending on whether if the strain reading is obtained from the surface or the internal part of the specimen. To recapitulate, stacking configuration affects damage state in the structures, and hence the strain readings of different sensors.

3.2.2 Relaxation of Compressive Residual Strain

Another interesting point that can be noted particularly from Figure 4(d)-(f) is that the lateral strains measured by the strain gage and FBG sensor acquire positive values under zero loading, which was also reported in [5, 6] without any discussion on possible physical reason, and considered to be a peculiar behavior in sensor reading. It is inferred that this is due to the relaxation of the curing induced compressive strain in both axial and lateral directions due to the transversal crack formation discussed in the previous section. The magnitude of the positive lateral strain increases with the cycle number. Specifically, as seen from Figure 4(f) belonging to the specimen with four off-axis plies, the lateral FBG strains under zero loading condition for the third, fourth and fifth and last cycles are 95, 110 and 145 and 384 $\mu\varepsilon$ respectively. Figure 4(f) also reveals that, after the fourth cycle, lateral strain of strain gage decreases with respect to the previous cycle, although the corresponding axial strain increases. One may argue that this can be due to the malfunctioning or debonding of the strain gage. However, given that the strain gage utilized is a rosette type biaxial strain gage, if there were such debonding, the axial strain would have indicated an off-track trend. The notable deviation in the strain gage recorded lateral strain after the 4^{th} cycle might be attributed to the extensive transversal cracks. It is noted that the extensometer due to its larger gage length is not as sensitive to the relaxation of the curing induced compressive strain as the other two local sensors.

3.2.3 The Variation of the Poisson's Ratio under Quasi-Static Cyclic Loading

Figure 5 presents the evolution of Poisson's ratio under quasi-static cyclic loading determined using the strain readings of three different sensor systems for specimens with three different ply stacking configurations in a matrix form with the row for the sensor type and the column for the stacking sequence. For the G6B1 plate in Figure 5 (a), each sensor system indicates the same decreasing trend in Poisson's ratio. It is worth noting that the Poisson's ratio of each subsequent cycle follows a different path from the previous cycle, except the first two cycles because the applied load has not induced sufficient damage to cause a change in the path of Poisson's ratio. After the second cycle, the applied axial strain can create sufficient transverse cracks and damage in composite materials, and thus Poisson's ratio follows a dissimilar path to the previous cycles. As the axial load is incremented, the Poisson's ratio gets a smaller maximum value, and also the difference between maximum and minimum values of Poisson's ratio decreases. This is attributed to the fact that, on the formation and accumulation of transverse cracks, the axial strain cannot be transferred in the lateral direction and, therefore, the lateral strain for a given axial strain decreases with respect to the previous cycle. Unlike strain gage or extensometer, which measures average strain fields across their gage length, thus not being notably influenced by local strain variations, the Poisson's ratio based on the strain field of the embedded biaxial FBG sensor is wavier. This stems from the irregular nature of the lateral FBG strain, as discussed previously. The waviness is more observable in the initial loading cycles since the damage generation rate is faster in these cycles. In later cycles, the rate of new damage formation decreases and the strain state of the structure does not change considerably, thereby leading to less momentous variation in the Poisson's ratio. At subsequent cycles, for lower axial strain levels, Poisson's ratio calculated using strain values of strain gage and FBG sensor possesses negative value due to positive lateral strain under the zero load due to the relaxed compressive strain.

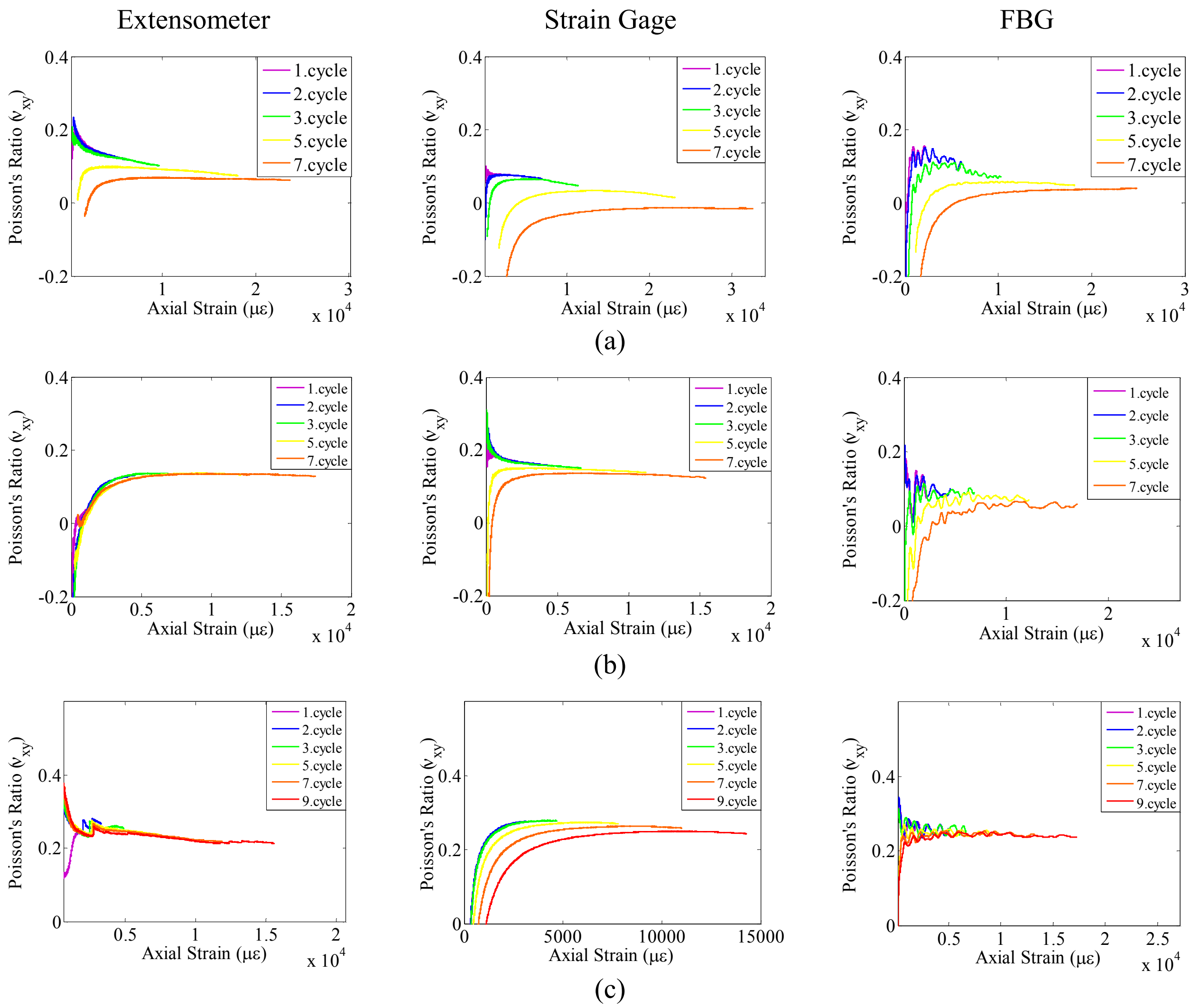

Figure 5: The evolution of Poisson's ratio under cyclic loading monitored based on the strain fields acquired by three different sensor systems for three different stacking sequences, namely, a) G6B1, b) G6B2, and c) G6U1, given row-wise ordering.

Comparing the results in Figure 5 in terms of stacking sequences, one can easily note that the Poisson' ratio increases as the number of 90^o plies decreases, as expected. The drop in the Poisson' ratio between the first and the final loading increases as the number of 90^o plies increases, indicating that 90^o plies are contributing to the formation of transverse cracks. Recalling that the specimens of the G6U1 plate are composed of completely unidirectional fibers, they do not allow for the formation of transverse cracking as much as the other two configurations, G6B1, and G6B2. Therefore, there is no significant change in the Poisson's ratio of each loading cycle for the specimen from the G6U1 plate, as seen in Figure 5(c). Figure 5(b) presents the Poisson's ratio of the specimen from G6B2 plate which has two off-axis plies. It is clear that, when off-axis plies are added to glass fiber reinforced composite, there is more deviation in the Poisson's ratio between subsequent cycles. The specimen from the G6B1 plate is more prone to transverse cracking and, therefore, it is expected that the difference between the Poisson's ratios of subsequent cycles should be largest for the specimen of G6B1 in comparison to the specimens from G6U1 and G6B2, as can be seen in Figure 5(a).

4. Concluding Remarks

The measurement of Poisson's ratio of composite materials using different types of surface-mounted strain sensors has been reported in the open literature. There are also several studies that describe the embedding of FBG sensors into composite materials for the measurement of axial strains [10]. However, there is no systematic study that addresses the effect of stacking sequence on the extent of lowering of Poisson's ratio. The work presented in this paper presents a new sensing approach to monitoring the evolution of Poisson's ratio based on strain data acquired using embedded multi-axis fiber optic sensors with the capability to measure both axial and transversal strains at the very same location from single fiber optic cable simultaneously. To this end, composites specimens with three different stacking sequences were mechanically tested under both static and quasi-static tensile loading. For comparison and validation, the decreasing trend in Poisson's ratio as a function of the axial strain was monitored using embedded biaxial FBG sensor, biaxial strain gage and dual extensometer. The following conclusions were can be drawn from this study:

a) When changing the layer number of off-axis plies, the Poisson ratio indicates a different evolution trend with respect to the applied strain. As the number of off-axis plies increases, a greater decline in the point by point evolution of Poisson's ratio is obtained;
b) Due to the formation of transverse cracks that hinder the effective transfer of axial load to the lateral direction and help the release of compressive strain, the transverse strain raises at a progressively smaller amount with increase in the applied load. This is the reason behind the decreasing trend in Poisson's ratio during the quasi-static tensile and quasi-static cyclic tension tests.
c) The embedded biaxial FBG sensors allow for tracking the variation of Poisson's ratio reliably and accurately;
d) The embedded biaxial FBG sensors are capable of capturing the damage state of composites through using reduction of Poisson's ratio as a damage index;
e) The embedded transverse FBG sensors are able to detect the effect of residual compressive strain relaxation on the measured lateral strain ;
f) The strain field in composite structures is sensitive to cracks, and the measured strain level is greatly influenced by the location, the gage length, and the type of the sensor;
g) Regardless of the difference in strain field acquired by three different sensor systems, it is shown that Poisson's ratio can be used as a reliable damage index since it is not based on the absolute value of the strain fields.

Acknowledgments: The authors gratefully acknowledge the funding provided by The Scientific and Technological Research Council of Turkey (TUBITAK), and Ministry of Science, Industry and Technology of Turkey for the project, 112M357, and 01307.STZ.2012-1, respectively.

References

[1] A.L. Highsmith, K.L. Reifsnider, Stiffness-reduction mechanisms in composite laminates, Damage in composite materials, 775 (1982) 103-117.
[2] F. Gao, L. Boniface, S. Ogin, P. Smith, R. Greaves, Damage accumulation in woven-fabric CFRP laminates under tensile loading: Part 1. Observations of damage accumulation, Composites science and technology, 59 (1999) 123-136.
[3] M. Surgeon, E. Vanswijgenhoven, M. Wevers, O. Van Der Biest, Transverse cracking and Poisson's ratio reduction in cross-ply carbon fibre-reinforced polymers, Journal of Materials Science, 34 (1999) 5513-5517.
[4] W. Van Paepegem, I. De Baere, E. Lamkanfi, J. Degrieck, Poisson's ratio as a sensitive indicator of (fatigue) damage in fibre-reinforced plastics, Fatigue & Fracture of Engineering Materials & Structures, 30 (2007) 269-276.
[5] I. De Baere, W. Van Paepegem, J. Degrieck, On the nonlinear evolution of the Poisson's ratio under quasi-static loading for a carbon fabric-reinforced thermoplastic. Part I: Influence of the transverse strain sensor, Polymer Testing, 28 (2009) 196-203.
[6] W. Van Paepegem, I. De Baere, E. Lamkanfi, J. Degrieck, Monitoring quasi-static and cyclic fatigue damage in fibre-reinforced plastics by Poisson's ratio evolution, International Journal of Fatigue, 32 (2010) 184-196.
[7] R. Pidaparti, A. Vogt, Experimental investigation of Poisson's ratio as a damage parameter for bone fatigue, Journal of biomedical materials research, 59 (2002) 282-287.
[8] P.A. Smith, J.R. Wood, Poisson's ratio as a damage parameter in the static tensile loading of simple crossply laminates, Composites Science and Technology, 38 (1990) 85-93.
[9] M. Yildiz, N.G. Ozdemir, G. Bektas, C.J. Keulen, T. Boz, E.F. Sengun, C. Ozturk, Y.Z. Menceloglu, A. Suleman, An experimental study on the process monitoring of resin transfer molded composite structures using fiber optic sensors, Journal of Manufacturing Science and Engineering, 134 (2012) 044502.
[10] C.J. Keulen, E. Akay, F.F. Melemez, E.S. Kocaman, A. Deniz, C. Yilmaz, T. Boz, M. Yildiz, H.S. Turkmen, A. Suleman, Prediction of fatigue response of composite structures by monitoring the strain energy release rate with embedded fiber Bragg gratings, Journal of Intelligent Material Systems and Structures, (2014) 1045389X14560358.
[11] E.S. Kocaman, C.J. Keulen, E. Akay, M. Yildiz, H.S. Turkmen, A. Suleman, An experimental study on the effect of length and orientation of embedded FBG sensors on the signal properties under fatigue loading, Science and Engineering of Composite Materials.
[12] C.J. Keulen, M. Yildiz, A. Suleman, Multiplexed FBG and etched fiber sensors for process and health monitoring of 2-&3-D RTM components, Journal of Reinforced Plastics and Composites, 30 (2011) 1055-1064.